Research Square

Preprints are preliminary reports that have not undergone peer review.
They should not be considered conclusive, used to inform clinical practice,
or referenced by the media as validated information.

Development and External Validation of a Risk Prediction Model for Hyperuricemia in Adolescents: A Multicenter Clinical Study

Zixing Wu
The Affiliated Yongchuan Hospital of Chongqing Medical University
Dan Liu
The Ninth People's Hospital of Chongqing
Xun Li
The Affiliated Yongchuan Hospital of Chongqing Medical University
Yuqiao Tang
Northeastern University
Ruitao Min
The Second Affiliated Hospital of Chongqing Medical University
Yunkai Mu
The Affiliated Yongchuan Hospital of Chongqing Medical University
Guibo Feng
fgbcqmu@163.com

The Affiliated Yongchuan Hospital of Chongqing Medical University

Article

Keywords: hyperuricemia, adolescents, risk prediction model, nomogram, external validation, health examination

Posted Date: April 6th, 2026

DOI: https://doi.org/10.21203/rs.3.rs-9168846/v1

License: This work is licensed under a Creative Commons Attribution 4.0 International License.
Read Full License

Additional Declarations: No competing interests reported.

Abstract

Hyperuricemia is increasingly prevalent among adolescents and is associated with metabolic disorders and future cardiovascular risk, yet risk prediction tools for this population remain limited. We developed and externally validated a multivariable prediction model for adolescent hyperuricemia using routinely collected health examination data. A total of 903 adolescents aged 12–18 years from two centers in Chongqing, China, were included, with 747 individuals for model development and 156 for external validation. Candidate variables were screened by univariate analysis and incorporated into a multivariable logistic regression model using Akaike information criterion -based selection. Model performance was evaluated in terms of discrimination, calibration, Brier score, and clinical utility using decision curve analysis. Eight predictors were retained, including body mass index, alkaline phosphatase, urea, red blood cell count, hemoglobin, γ-glutamyl transferase, absolute monocyte count, and absolute neutrophil count. Discrimination was maintained across datasets, with AUCs of 0.831 in development and 0.804 in external validation, while Brier scores were 0.142 and 0.194, respectively, indicating overall adequate model performance. Decision curve analysis further suggested net clinical benefit across low-risk thresholds. The model provides individualized risk estimates and may facilitate early identification and risk stratification of hyperuricemia in adolescents.

Introduction

Hyperuricemia is a common metabolic disorder that not only leads to gout but is also closely associated with obesity, insulin resistance, metabolic syndrome, and cardiovascular disease. (1) In recent years, epidemiological studies from multiple regions in China have reported a prevalence of hyperuricemia ranging from 10% to > 30% among children and adolescents, suggesting that uric acid–related metabolic risk may begin to increase as early as adolescence. (2)

However, this issue is often overlooked, and existing studies in adolescent populations have largely focused on descriptive epidemiology and risk factor identification or have extrapolated prediction models originally developed in adult cohorts. As a result, risk prediction tools specifically designed for adolescents remain limited.

Importantly, serum uric acid (SUA) levels in adolescents are influenced by their developmental stage and metabolic status, and the constellation of risk factors for hyperuricemia may therefore differ from those observed in adults. (2, 3) Direct application of adult-based prediction models may thus fail to adequately capture risk profiles specific to adolescents. These considerations highlight the need for risk prediction models for hyperuricemia tailored to this population.

Accordingly, the present study aimed to develop and externally validate a risk prediction model for hyperuricemia in adolescents using clinical and biochemical parameters routinely available from health examination settings, with the goal of supporting early risk screening and health management in both health check-up and primary care contexts.

Methods

Study Population

This retrospective cross-sectional study included adolescents meeting the following criteria: (1) individuals who underwent routine health examinations at the Health Examination Centers of Beibei Hospital and Yongchuan Hospital affiliated with Chongqing Medical University between January 2023 and December 2024; (2) age 12–18 years; and (3) completion of fasting blood biochemical and routine hematological tests.

The exclusion criteria were as follows: (1) missing key indicators such as serum uric acid; (2) a prior diagnosis of severe cardiovascular, hepatic, renal, or hematological diseases; (3) duplicate examination records; (4) use of medications known to affect SUA levels, such as diuretics or allopurinol; and (5) laboratory results considered implausible after manual review. A total of 903 adolescents were included in the final analysis.

This retrospective cross-sectional study was approved by the Ethics Committees of Beibei Hospital and Yongchuan Hospital affiliated with Chongqing Medical University (Approval No. 2025EC0245). As the study used anonymized data derived from routine health examinations and involved no direct contact with participants, the requirement for written informed consent was waived by the ethics committees.

Definition of Hyperuricemia

At present, no universally accepted diagnostic criteria for hyperuricemia in adolescents are available. In accordance with the latest Chinese clinical practice consensus, adult diagnostic thresholds are recommended as a reference, with hyperuricemia defined as an SUA concentration ≥ 420 μmol/L on two separate occasions. Given that routine health examinations typically provide only a single fasting blood sample, hyperuricemia in the present study was defined as an SUA concentration ≥ 420 μmol/L for subsequent risk prediction analyses (2, 4).

Data Collection and Outcome Definition

On the basis of previous studies and clinical interpretability, the following variables were considered: (1) demographic and anthropometric variables: sex, age, height, weight, body mass index (BMI), systolic blood pressure, and diastolic blood pressure; (2) metabolic and renal function indicators: urea, creatinine, SUA, homocysteine, glucose, total cholesterol, triglycerides, high-density lipoprotein cholesterol, low-density lipoprotein cholesterol, and apolipoprotein A1; (3) liver function indicators: alanine aminotransferase (ALT), aspartate aminotransferase (AST), γ-glutamyl transferase (GGT), alkaline phosphatase (ALP), and total bilirubin; (4) hematologic and inflammatory indicators: white blood cell count (WBC), neutrophil percentage and absolute neutrophil count (NAbs), monocyte percentage and absolute monocyte count (MAbs), red blood cell count (RBC), platelet count, and hemoglobin (HB); (5) urinalysis indicators: urine pH, urine specific gravity, urine protein, and urine glucose.

At Beibei Hospital affiliated with Chongqing Medical University, routine hematological tests were performed using a Mindray BC-6000 automated hematology analyzer, and biochemical parameters were measured using a Hitachi 008AS automated biochemical analyzer. At Yongchuan Hospital affiliated with Chongqing Medical University, routine hematological tests were performed using a Mindray BC-7500 automated hematology analyzer, and biochemical parameters were measured using a Siemens XPT automated biochemical analysis system. The clinical laboratories of both hospitals are accredited by the national clinical laboratory quality control system, and all laboratory tests were conducted in accordance with standardized clinical laboratory procedures.

The primary outcome was the presence of hyperuricemia (SUA ≥ 420 μmol/L), which was treated as a binary dependent variable for subsequent model development.

Statistical Analysis

Missing data were handled according to the proportion of missingness for each variable. For continuous variables with a missing rate of < 10% (including NAbs, BMI, SBP, DBP, ALP, GGT, WBC, RBC, HB, ALT, and AST), median imputation was applied, whereas categorical variables were imputed using the mode (e.g., sex). Continuous variables with a missing rate of > 30% (urine pH, urine specific gravity, urine protein, and urine glucose) were excluded from model construction to avoid potential bias due to excessive imputation.

Restricted cubic spline (RCS) analysis was used to evaluate the dose–response relationship between continuous variables and the risk of hyperuricemia and to test for potential nonlinear trends. In addition, stepwise covariate-adjusted regression models were used to evaluate the attenuation of center effects.

Model Development

The Beibei cohort was used as the training dataset. Univariable analyses were first performed to screen for variables significantly associated with hyperuricemia ($P < 0.05$). These variables were then included in a multivariable logistic regression model, with backward stepwise selection based on the AIC. A nomogram was constructed on the basis of the regression coefficients to facilitate individualized risk prediction. A web-based dynamic nomogram was also developed to facilitate interactive risk estimation.

Internal Validation

Internal validation was conducted using bootstrap resampling with 1,000 iterations to obtain optimism-corrected estimates of model performance. Discrimination was assessed using the area under the receiver operating characteristic curve (AUC) and the concordance index (C-index). Calibration was evaluated using calibration plots, the Brier score, the calibration intercept and slope (overall calibration), as well as Emax, E90, and Eavg. The Hosmer–Lemeshow goodness-of-fit test was used as a supplementary assessment. The logistic calibration line, LOESS-smoothed curve, and ideal reference line

from the calibration plots were used to visually assess the agreement between the predicted and observed probabilities.

External Validation

The final model derived from the training dataset was applied to the Yongchuan cohort to generate predicted probabilities. Model performance in the external validation cohort was assessed using the AUC, Brier score, Hosmer–Lemeshow test, and calibration metrics including Emax, E90, and Eavg. Clinical net benefit was evaluated using decision curve analysis (DCA).

Data Analysis

All the statistical analyses were performed using R software version 4.5.1 (R Foundation for Statistical Computing, Vienna, Austria), primarily employing the rms, pROC, and ggplot2 packages. Continuous variables are summarized as the mean ± standard deviation (SD) or median (interquartile range, IQR), depending on the data distribution, whereas categorical variables are presented as counts and percentages. Group comparisons are conducted using Student's t-test, the Mann–Whitney U test, or the χ^2 test as appropriate. All the statistical tests were two-tailed, and a P value < 0.05 was considered to indicate statistical significance. Continuous variables were included in the analysis as original values without categorization in order to preserve their continuity.

Results

Baseline Characteristics

During the study period, 5,138 individuals undergoing health examinations were screened. After applying the exclusion criteria, a total of 903 adolescents were included in the final analysis. Of these, 747 from Beibei served as the training cohort for model development and internal validation, and 156 from Yongchuan constituted an independent external validation cohort (Fig. 1).

The overall prevalence of hyperuricemia (SUA ≥ 420 μmol/L) was 32.0%, with rates of 28.1% in Beibei and 50.6% in Yongchuan. There were no significant differences between the two centers in terms of sex and age distribution; however, serum uric acid levels were significantly higher in the Yongchuan cohort than in the Beibei cohort. The baseline demographic and clinical laboratory characteristics of the two groups are presented in Table 1.

Table 1

A. Baseline characteristics of adolescents in Beibei cohort

Variable	Non-HUA (n = 537)	HUA (n = 210)	P value
Hyperuricemia (%)	28.1%		
Age (years)	12 (12, 15)	15 (12, 15)	< 0.001
Male, n (%)	174 (32.4%)	172 (81.9%)	< 0.001
Female, n (%)	363 (67.6%)	38 (18.1%)	
Height (cm)	159.0 (154.0, 164.0)	166.5 (159.5, 171.5)	< 0.001
Weight (kg)	48.0 (42.0, 56.0)	61.0 (51.0, 75.0)	< 0.001
BMI (kg/m^2)	18.9 (17.1, 21.6)	22.9 (19.1, 26.8)	< 0.001
SBP (mmHg)	110 (100, 120)	117 (107, 127)	< 0.001
DBP (mmHg)	67 (62, 74)	70 (64, 76)	< 0.001
Urea (mmol/L)	3.84 (3.18, 4.55)	4.28 (3.60, 5.16)	< 0.001
Creatinine (umol/L)	54 (46, 63)	64 (53, 74)	< 0.001
ALT (U/L)	11 (9, 15)	18 (11, 28)	< 0.001
AST (U/L)	18 (16, 21)	20 (17, 26)	< 0.001
GGT (U/L)	12 (10, 16)	18 (13, 29)	< 0.001
ALP (U/L)	151 (99, 240)	173 (125, 255)	< 0.001
WBC (10^9/L)	6.52 (5.58, 7.71)	6.84 (6.02, 7.98)	0.006
Neutrophil (%)	53.1 (46.7, 58.0)	52.2 (47.0, 57.3)	0.614
Neutrophil (10^9/L)	3.40 (2.67, 4.24)	3.67 (2.83, 4.51)	0.064
Monocyte (%)	5.1 (4.4, 5.9)	5.4 (4.7, 6.1)	0.006
Monocyte (10^9/L)	0.33 (0.27, 0.41)	0.37 (0.31, 0.45)	< 0.001
RBC (10^12/L)	4.92 (4.66, 5.17)	5.28 (4.98, 5.54)	< 0.001
Platelet (10^9/L)	274 (235, 313)	276 (244, 315)	0.132
Hemoglobin (g/L)	141 (134, 148)	150 (142, 160)	< 0.001
Urine protein, n (%)	19 (3.5%)	4 (1.9%)	0.346

Values are presented as median (IQR) or n (%). BMI, body mass index; SBP, systolic blood pressure; DBP, diastolic blood pressure; ALT, alanine aminotransferase; AST, aspartate aminotransferase; GGT, gamma-glutamyl transferase; ALP, alkaline phosphatase; WBC, white blood cell; RBC, red blood cell.

Table 1
B. Baseline characteristics of adolescents in Yongchuan cohort

Variable	Non-HUA (n = 77)	HUA (n = 79)	P value
Hyperuricemia (%)	50.6%		
Age (years)	16 (15, 17)	16 (15, 17)	0.275
Male, n (%)	30 (39.0%)	71 (89.9%)	< 0.001
Female, n (%)	47 (61.0%)	8 (10.1%)	
Height (cm)	164.0 (160.0, 171.0)	172.0 (168.0, 179.0)	< 0.001
Weight (kg)	55.1 (47.4, 69.3)	72.1 (58.0, 85.4)	< 0.001
BMI (kg/m^2)	20.6 (18.0, 23.2)	24.1 (19.9, 28.5)	< 0.001
SBP (mmHg)	108 (98, 119)	118 (109, 132)	< 0.001
DBP (mmHg)	65 (61, 71)	68 (61, 76)	0.294
Urea (mmol/L)	4.22 (3.62, 5.16)	4.67 (4.10, 5.56)	0.055
Creatinine (umol/L)	62 (54, 69)	75 (68, 81)	< 0.001
ALT (U/L)	13 (10, 18)	26 (15, 51)	< 0.001
AST (U/L)	19 (16, 21)	23 (18, 32)	< 0.001
GGT (U/L)	16 (12, 20)	27 (20, 49)	< 0.001
ALP (U/L)	99 (83, 127)	108 (92, 162)	0.126
WBC (10^9/L)	6.30 (5.20, 7.30)	6.70 (5.60, 7.70)	0.085
Neutrophil (%)	52.8 (48.6, 57.7)	56.5 (48.6, 61.3)	0.049
Neutrophil (10^9/L)	3.40 (2.67, 4.04)	3.92 (2.77, 4.91)	0.038
Monocyte (%)	6.1 (5.0, 6.9)	6.1 (5.2, 7.5)	0.382
Monocyte (10^9/L)	0.37 (0.31, 0.45)	0.41 (0.36, 0.52)	0.031
RBC (10^12/L)	4.89 (4.50, 5.33)	5.41 (5.10, 5.68)	< 0.001
Platelet (10^9/L)	282 (235, 303)	254 (225, 303)	0.201
Hemoglobin (g/L)	145 (129, 153)	157 (148, 164)	< 0.001
Urine protein, n (%)	7 (9.1%)	9 (11.4%)	0.793

Values are presented as median (IQR) or n (%). BMI, body mass index; SBP, systolic blood pressure; DBP, diastolic blood pressure; ALT, alanine aminotransferase; AST, aspartate aminotransferase; GGT, gamma-glutamyl transferase; ALP, alkaline phosphatase; WBC, white blood cell; RBC, red blood cell.

Internal Validation

In the Beibei training cohort, the AUC was 0. 831 (95% CI: 0.798–0.863) (Fig. 2).

In terms of calibration, the Brier score was 0.142 and the Hosmer–Lemeshow test yielded P = 0.582. Calibration error metrics were Emax = 0.066, E90 = 0.032, and Eavg = 0.013. The internal calibration curve (Fig. 3A) showed good agreement between the predicted probabilities and the observed outcomes.

External Validation

In the Yongchuan validation cohort, the AUC was 0.804 (95% CI: 0.736–0.873) (Fig. 2). The Brier score was 0.194, and the Hosmer–Lemeshow test yielded P = 0.007. The calibration error metrics were Emax = 0.167, E90 = 0.158, and Eavg = 0.093. The external calibration curve (Fig. 3B) showed a tendency toward underestimation in the higher predicted risk range, whereas the overall calibration trend remained consistent across the main distribution of predicted probabilities.

Decision curve analysis (Fig. 4) demonstrated that, within the low-risk threshold range relevant for screening and early intervention, the model provided greater net benefit than the “treat-none” strategy.

Model Development

After multivariable logistic regression with backward stepwise selection based on the AIC, eight variables were retained in the final prediction model: BMI, ALP, urea, RBC, HB, GGT, MAbs, and NAbs. A nomogram for predicting the risk of hyperuricemia in adolescents was constructed on the basis of these predictors (Fig. 5).

In the static nomogram, BMI and GGT showed relatively high regression weights. In addition, a web-based dynamic nomogram (Fig. 6) was developed based on this model to present individualized risk predictions.

Dose–Response Relationship Analysis

Restricted cubic spline analysis showed that BMI was significantly and positively associated with the risk of hyperuricemia (P overall < 0.001), with no evident nonlinear trend (P nonlinearity = 0.58)(Fig. 7A). GGT was also significantly associated with the risk of hyperuricemia (P overall = 0.0047) and showed a marginal nonlinear trend (P nonlinearity = 0.0848) (Fig. 7B).

Center Effect Analysis

Stepwise covariate-adjusted analyses showed that the center effect between Yongchuan and Beibei gradually attenuated after sequential adjustment for age, obesity and blood pressure indicators, renal function indicators, and hepatic metabolic indicators, and was no longer statistically significant in the fully adjusted model.

Discussion

In this study, we developed and externally validated a multivariable risk prediction model for hyperuricemia in adolescents using data from two health examination centers in Chongqing, China, supporting early identification and risk stratification of hyperuricemia in adolescents. Decision curve analysis showed that the model yielded net benefit within low-risk threshold ranges, indicating its potential application in screening and risk stratification for adolescent hyperuricemia. In addition, a web-based dynamic nomogram developed based on this model improved the feasibility of individualized risk assessment.

A marked disparity in hyperuricemia prevalence was observed between the Beibei and Yongchuan cohorts (28.1% vs. 50.6%). Previous studies have reported substantial regional heterogeneity in SUA levels among adolescents in China, with dietary patterns, lifestyle behaviors, and obesity levels considered important contributing factors (2, 5). Although lifestyle-related variables such as diet and physical activity were not included in the present study, limiting the depth of interpretation, the regional differences observed are generally consistent with previous epidemiological evidence.

To further explore the potential sources of these regional differences, we conducted stepwise covariate-adjusted analyses to evaluate changes in the center effect. The results showed that after sequential adjustment for age, obesity and blood pressure indicators, renal function indicators, and hepatic metabolic indicators, the center effect gradually attenuated and was no longer statistically significant in the fully adjusted model. These findings suggest that the difference in prevalence between the two regions may be related to differences in the metabolic profiles of the populations. However, some degree of miscalibration in the higher-risk range was still observed in the external validation, indicating that regional differences in risk distribution may continue to influence model performance. Therefore, when developing and applying multicenter prediction models, population structure differences should be carefully considered, and further validation in broader geographic populations is warranted to assess the generalizability of the model.

During variable selection, several indicators such as ALT, AST, and creatinine also showed statistical differences; however, they were not retained in the final model after multivariable analysis combined with backward stepwise selection based on the AIC. This suggests that these variables may share overlapping information with predictors already included in the model, and their independent predictive value may be relatively limited within the multivariable framework, and therefore were not included in the final model. In the final model, BMI and GGT showed relatively higher contributions. Restricted cubic spline analysis showed that BMI was linearly and positively associated with the risk of hyperuricemia (P overall < 0.001, P for nonlinearity = 0.58), with no evident threshold or U-shaped relationship observed, indicating that the risk increased progressively with increasing BMI. This linear relationship suggests that, in adolescents, incorporating BMI as a continuous variable in risk assessment may provide more information than using a single obesity cutoff. GGT was also significantly associated with the risk of hyperuricemia (P overall = 0.0047) and showed a marginal nonlinear trend (P for nonlinearity = 0.0848),

with the risk increasing more noticeably within the low-to-moderate GGT range. Combined with the results of decision curve analysis, the model demonstrated relative net benefit compared with the “treat-none” strategy within a threshold probability range of approximately 0.10–0.25. With other variables held constant, the predicted risk reached approximately 10% when GGT was around 14 U/L and approached 20%–25% when GGT was approximately 20–30 U/L. Within the model framework, the risk showed an increasing trend when GGT exceeded approximately 20 U/L, which may provide a reference range for risk stratification. It should be emphasized that these ranges represent conditional risk stratification estimated from the model rather than biological thresholds. Nevertheless, these key variables themselves have clear biological relevance, and their potential links with uric acid metabolism warrant further discussion.

From a biological perspective, the eight predictors included in this study are clearly related to key physiological pathways involved in uric acid metabolism. First, the metabolic–hepatic axis, represented by BMI, GGT, and ALP, reflects the combined influence of obesity, lipid metabolism, and oxidative stress on uric acid homeostasis. Obesity contributes to elevated SUA levels through insulin resistance and adipose tissue inflammation, and a stable positive association between BMI and SUA levels has been consistently reported (6–9). GGT, a well-recognized marker of oxidative stress and metabolic syndrome, is closely linked to hyperuricemia; increased GGT levels often indicate increased hepatic lipid burden and systemic oxidative stress, which may participate in the regulation of purine metabolism (10–12). Although ALP is not a traditional marker of hyperuricemia, it is frequently elevated in the context of insulin resistance and hepatobiliary metabolic disturbances (13, 14), and these metabolic abnormalities are also related to elevated uric acid levels (15, 16), potentially linking ALP with uric acid through similar metabolic pathways. Taken together, the inclusion of BMI, GGT, and ALP in the model is biologically plausible.

Second, urea, which represents the renal function–excretion axis, reflects the kidney’s capacity to handle metabolic byproducts. As a sensitive indicator of glomerular filtration, increased urea levels may indicate subtle changes in renal functional reserve or filtration efficiency (17). Previous studies suggest that even mild variations in renal function within the conventionally normal range may influence uric acid excretion through alterations in tubular reabsorption and secretion (18). Therefore, the inclusion of urea as a predictor may reflect an association between mild differences in renal function and uric acid excretory efficiency; these subtle variations may not constitute disease but may still influence uric acid homeostasis during adolescence (18, 19).

Third, the hematopoietic–purine load axis merits particular attention. Hematopoietic activity and nucleic acid turnover generate purine substrates that are ultimately metabolized to uric acid, providing a potential link between RBC and SUA levels (20, 21). Data from Chinese adult populations have demonstrated positive associations between RBC, hemoglobin, and SUA levels, which is consistent with our observations (22). Moreover, adolescence is characterized by physiologically increased hematopoietic activity, with marked increases in red blood cell–related parameters, particularly among males (23). This developmental feature offers a biological context for the inclusion of RBC and

hemoglobin as predictors in the model. Although current evidence does not establish a causal relationship, our findings suggest that hematopoietic activity may represent a relevant dimension of uric acid metabolism in adolescents.

Inflammatory and immune-related markers, represented by MAbs and NAbs, were also retained in the final model. Prior studies have demonstrated close links between obesity-related adipose inflammation, low-grade systemic inflammation, metabolic syndrome, and hyperuricemia. Composite inflammatory indices derived from neutrophil and monocyte parameters, such as the systemic immune-inflammation index (SII) and systemic inflammation response index (SIRI), have been associated with increased uric acid levels and adverse outcomes (9, 20, 24, 25). Experimental evidence further indicates that oxidative stress and inflammatory mediators can influence purine metabolism, renal tubular transport, and uric acid production and clearance (20, 25). The independent contribution of inflammatory markers in our model highlights the potential importance of metabolic–inflammatory interactions in the development of adolescent hyperuricemia.

Overall, the eight predictors incorporated into the model span multiple physiological domains, including lipid metabolism, hepatic function, renal excretion, hematopoietic activity, and the inflammatory response, forming a biologically coherent and integrative prediction framework. The physiological interconnections among these variables also provide a biological basis for the structure of the model.

Several limitations of this study should be acknowledged. First, hyperuricemia was defined on the basis of a single fasting SUA measurement, which may have introduced a degree of misclassification. Second, as the data were derived from routine health examination records, information on lifestyle factors such as diet, physical activity, and sugar-sweetened beverage consumption was unavailable, potentially resulting in residual confounding. Third, although external validation was performed, the validation cohort was relatively small and originated from the same geographic region (Chongqing), which may limit the generalizability of the model. Further validation in larger, multicenter cohorts across different regions is therefore warranted. In addition, because the sample size in the higher GGT range was relatively limited, the statistical stability of the nonlinear trend between GGT and hyperuricemia requires further verification in larger samples. Finally, owing to the retrospective study design, causal relationships between predictors and hyperuricemia cannot be inferred, and prospective multicenter studies are needed to further confirm the clinical utility of the model.

Abbreviations

AIC: Akaike information criterion; ALP: Alkaline phosphatase; ALT: Alanine aminotransferase; AST: Aspartate aminotransferase; AUC: Area under the receiver operating characteristic curve; BMI: Body mass index; CI: Confidence interval; DCA: Decision curve analysis; DBP: Diastolic blood pressure; GGT: Gamma-glutamyl transferase; HB: Hemoglobin; HUA: Hyperuricemia; IQR: Interquartile range; MAbs: Absolute monocyte count; NAbs: Absolute neutrophil count; OR: Odds ratio; RBC: Red blood cell count;

RCS: Restricted cubic spline; ROC: Receiver operating characteristic; SBP: Systolic blood pressure; SD: Standard deviation; SUA: Serum uric acid; WBC: White blood cell count

Declarations

Ethics Statement

This study was conducted in accordance with the Declaration of Helsinki and was approved by the Ethics Committees of Beibei Hospital and Yongchuan Hospital affiliated with Chongqing Medical University.

As this was a retrospective study based on anonymized health examination data, the requirement for written informed consent was waived by the ethics committees.

Consent for publication

Not applicable.

Author Contributions

ZW conceived the study, performed data curation and statistical analysis, and drafted the manuscript.

DL and XL contributed equally to this work and were responsible for data collection and data verification.

YT, RM, and YM contributed equally to this work and assisted with data interpretation and critical revision of the manuscript.

GF supervised the study, provided methodological guidance, and critically reviewed and revised the manuscript.

All authors read and approved the final manuscript.

Funding

The authors declare that this study received no external funding.

Competing interests

The authors declare that they have no competing interests.

Data Availability Statement

The datasets presented in this article are not readily available due to ethical and privacy restrictions.

Requests to access the datasets should be directed to the corresponding author.

Acknowledgments

The authors would like to thank the staff of the Health Examination Centers of Beibei Hospital and Yongchuan Hospital for their assistance with data collection.

References

1. Kubota, M. Hyperuricemia in children and adolescents: present knowledge and future directions. J. Nutr. Metab. 3480718 (2019). (2019).
2. Rao, J. et al. Prevalence and related factors of hyperuricaemia in Chinese children and adolescents: a pooled analysis of 11 population-based studies. *Ann. Med.* **54**, 1608–1615 (2022).
3. Ford, E. S., Li, C., Cook, S. & Choi, H. K. Serum concentrations of uric acid and the metabolic syndrome among US children and adolescents. *Circulation* **115**, 2526–2532 (2007).
4. Li, C. et al. Clinical practice consensus statement 2025: management of hyperuricemia and gout in adolescents. *Int. J. Rheum. Dis.* **28**, e70378 (2025).
5. Liu, R. et al. Prevalence of hyperuricemia and gout in mainland China from 2000 to 2014: a systematic review and meta-analysis. Biomed. Res. Int. 762820 (2015). (2015).
6. Niu, Y. et al. Obesity-induced insulin resistance is mediated by high uric acid in obese children and adolescents. *Front. Endocrinol.* **12**, 773820 (2021).
7. Dikker, O., Aktaş, A., Şahin, M., Doğan, M. & Dağ, H. The association of serum uric acid levels and various uric acid-related ratios with insulin resistance and obesity: a preliminary study in adolescents. *Children* **10**, 1579 (2023).
8. Cheng, L. et al. The associations of insulin resistance, obesity, and lifestyle with the risk of developing hyperuricaemia in adolescents. *BMC Endocr. Disord*. **24**, 220 (2024).
9. He, H. et al. Exercise effects on the link between inflammation, metabolic health and hyperuricemia: a prospective cohort study. *Lipids Health Dis.* **24**, 289 (2025).
10. Hernández-Rubio, A. et al. Association of hyperuricemia and gamma glutamyl transferase as a marker of metabolic risk in alcohol use disorder. *Sci. Rep.* **10**, 20060 (2020).
11. Lee, M. Y. et al. Association between serum gamma-glutamyltransferase and prevalence of metabolic syndrome using data from the Korean genome and epidemiology study. *Endocrinol. Metab.* **34**, 390–397 (2019).
12. Wang, Y. et al. Relationship between serum gamma-glutamyl transferase level and impaired fasting glucose among Chinese community-dwelling adults: a follow-up observation of 6 years. *Metab. Syndr. Relat. Disord*. **19**, 100–106 (2021).
13. Kim, J. H. et al. Serum alkaline phosphatase level is positively associated with metabolic syndrome: a nationwide population-based study. *Clin. Chim. Acta*. **500**, 189–194 (2020).
14. Yan, W. et al. Associations of serum alkaline phosphatase level with all-cause and cardiovascular mortality in the general population. *Front. Endocrinol.* **14**, 1217369 (2023).

15. Raya-Cano, E. et al. Association between metabolic syndrome and uric acid: a systematic review and meta-analysis. *Sci. Rep.* **12**, 18412 (2022).
16. Kanbay, M. et al. Uric acid in metabolic syndrome: from an innocent bystander to a central player. *Eur. J. Intern. Med.* **29**, 3–8 (2016).
17. Gounden, V., Bhatt, H. & Jialal, I. Renal function tests. StatPearls (StatPearls Publishing, Treasure Island, (2025).
18. Tsai, C. W., Lin, S. Y., Kuo, C. C. & Huang, C. C. Serum uric acid and progression of kidney disease: a longitudinal analysis and mini-review. *PLoS One*. **12**, e0170393 (2017).
19. Adeyomoye, O. I. et al. The biological roles of urea: a review of preclinical studies. *Indian J. Nephrol.* **32**, 539–545 (2022).
20. Du, L. et al. Hyperuricemia and its related diseases: mechanisms and advances in therapy. *Signal. Transduct. Target. Ther.* **9**, 212 (2024).
21. Dudzinska, W. et al. Comparison of human erythrocyte purine nucleotide metabolism and blood purine and pyrimidine degradation product concentrations before and after acute exercise in trained and sedentary subjects. *J. Physiol. Sci.* **68**, 293–305 (2018).
22. Su, P. et al. The association between hyperuricemia and hematological indicators in a Chinese adult population. *Medicine* **95**, e2822 (2016).
23. Mancera-Soto, E. M. et al. Hemoglobin mass, blood volume and VO_2max of trained and untrained children and adolescents living at different altitudes. *Front. Physiol.* **13**, 892247 (2022).
24. Ren, T. et al. Systemic inflammation markers independently associated with increased mortality in individuals with hyperuricemia: results from the NHANES prospective cohort study. *Immun. Inflamm. Dis.* **12**, e70032 (2024).
25. Masenga, S. K. et al. Mechanisms of oxidative stress in metabolic syndrome. *Int. J. Mol. Sci.* **24**, 7742 (2023).

Figures

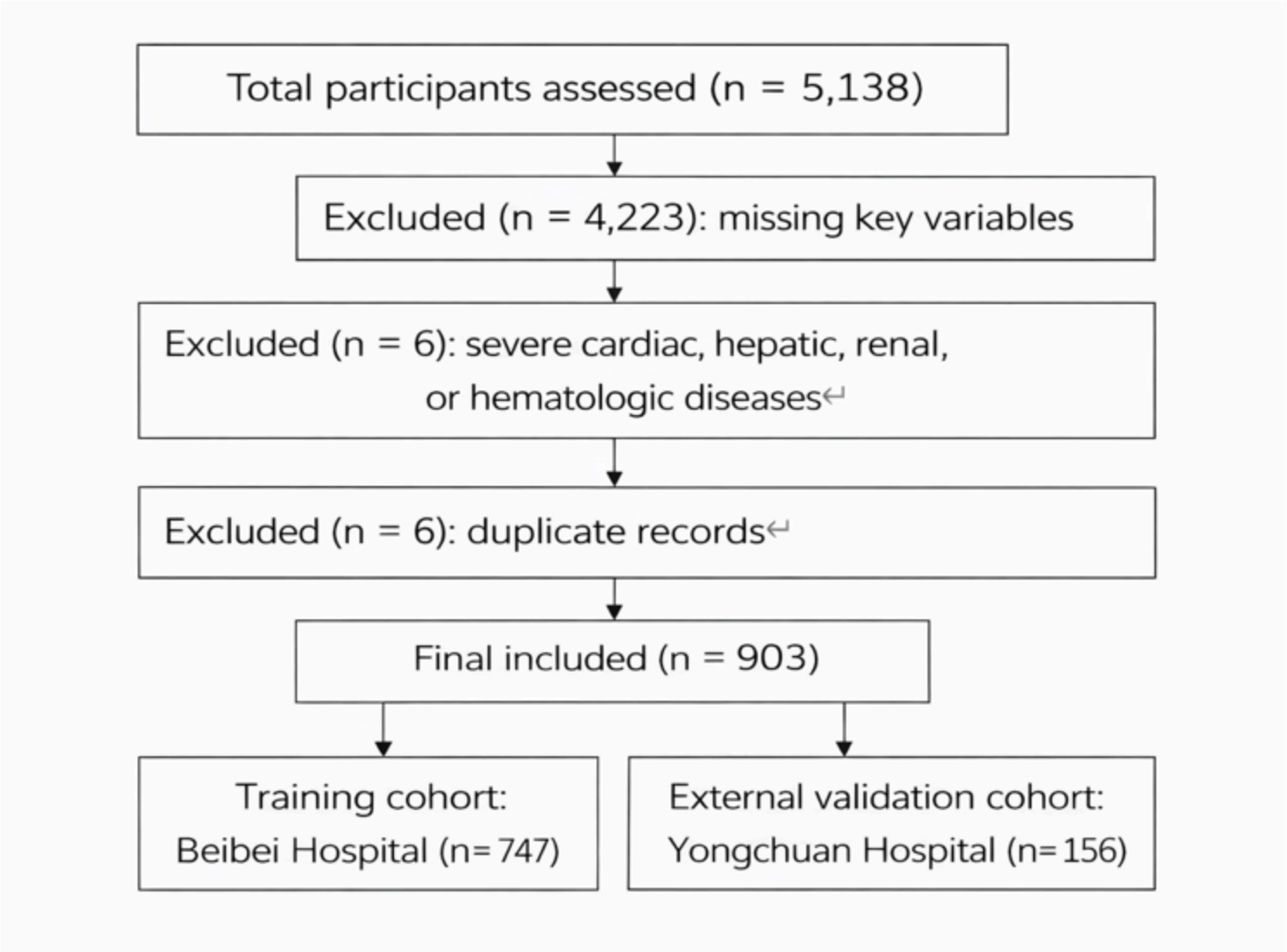


Figure 1

Study flow diagram.

Flowchart illustrating the participant selection process. A total of 5138 individuals undergoing routine health examinations were screened during the study period. After applying the exclusion criteria, 903 adolescents were included in the final analysis, of whom 747 from Beibei were used for model development and internal validation and 156 from Yongchuan served as the independent external validation cohort.

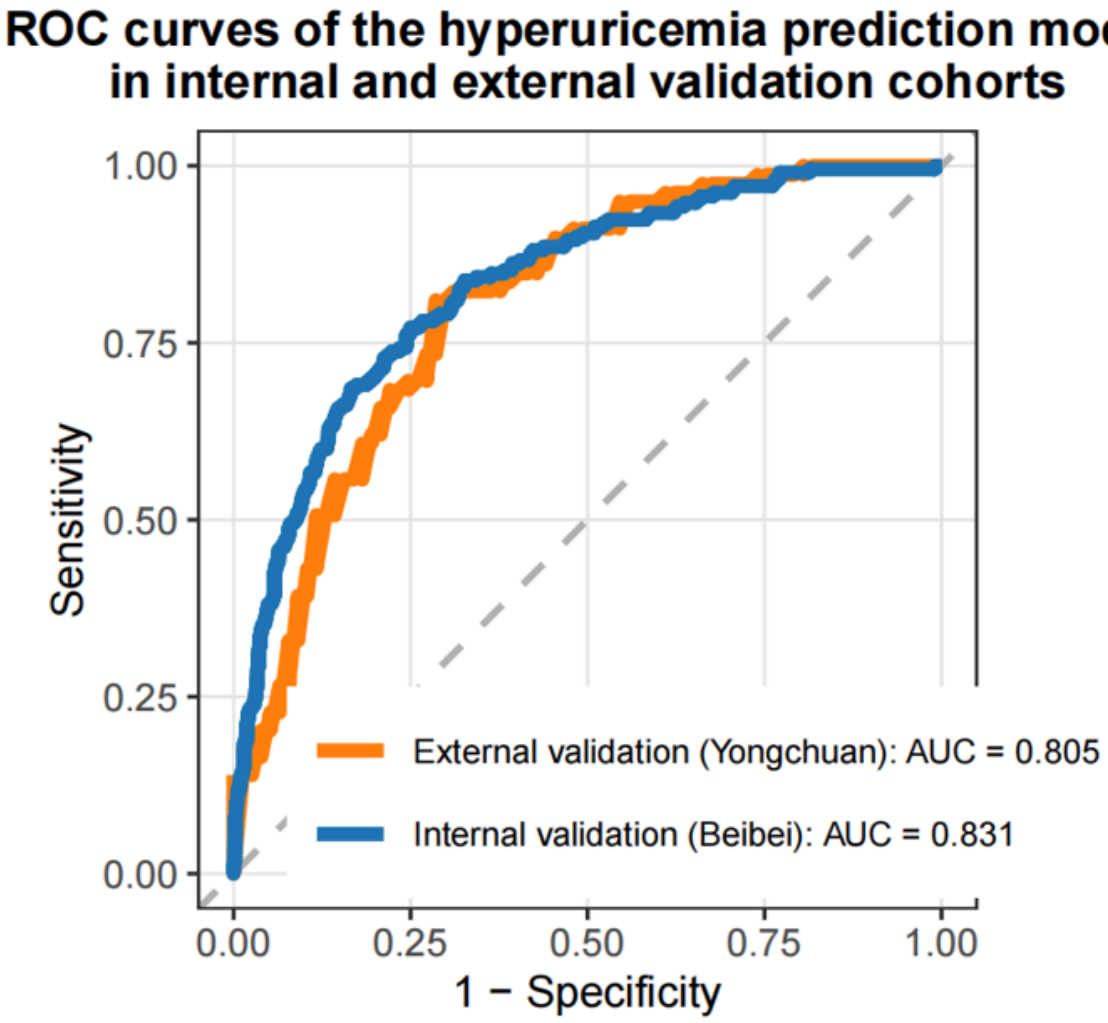


Figure 2

Receiver operating characteristic (ROC) curves of the prediction model.
ROC curves illustrating the discrimination performance of the hyperuricemia risk prediction model in the Beibei training cohort and the Yongchuan external validation cohort. The area under the curve (AUC) values reflect the discriminatory ability of the model in both datasets.

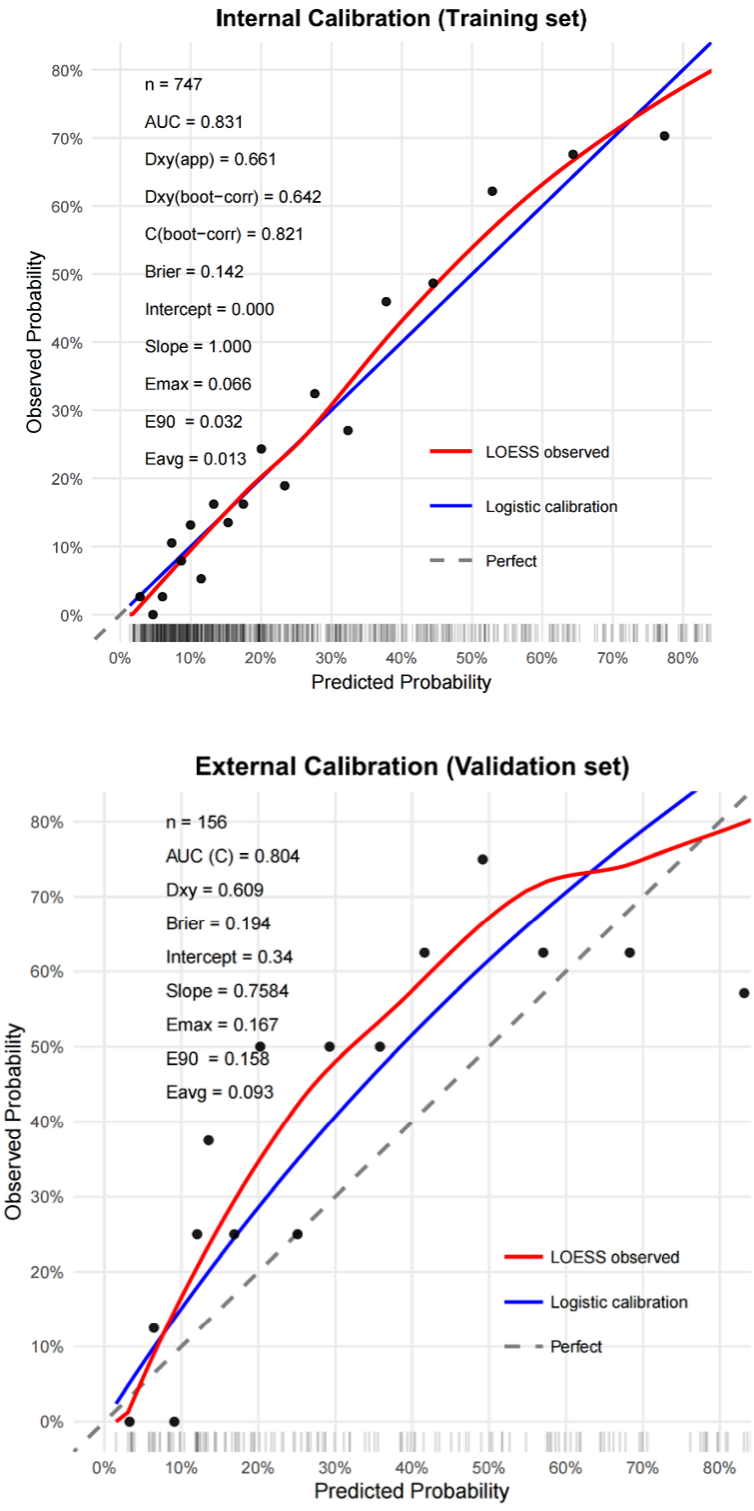


Figure 3

Calibration curves of the prediction model.

Calibration plots showing the agreement between predicted probabilities and observed outcomes in the (A) training cohort and (B) external validation cohort. The solid line represents the model calibration, and the dashed line indicates the ideal reference line.

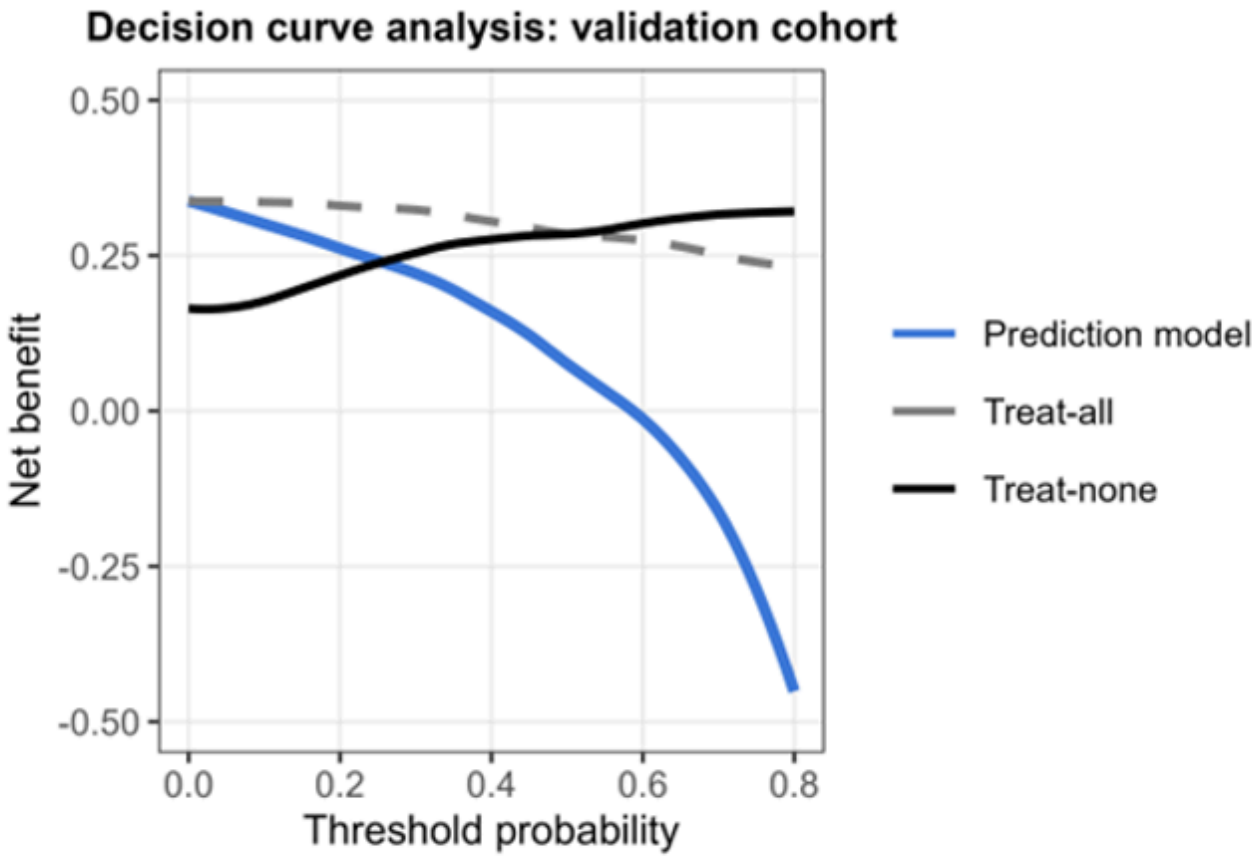


Figure 4

Decision curve analysis (DCA) of the prediction model.
Decision curve analysis evaluating the clinical net benefit of the prediction model across a range of threshold probabilities. The model demonstrated greater net benefit than the “treat-none” strategy within clinically relevant low-risk threshold ranges.

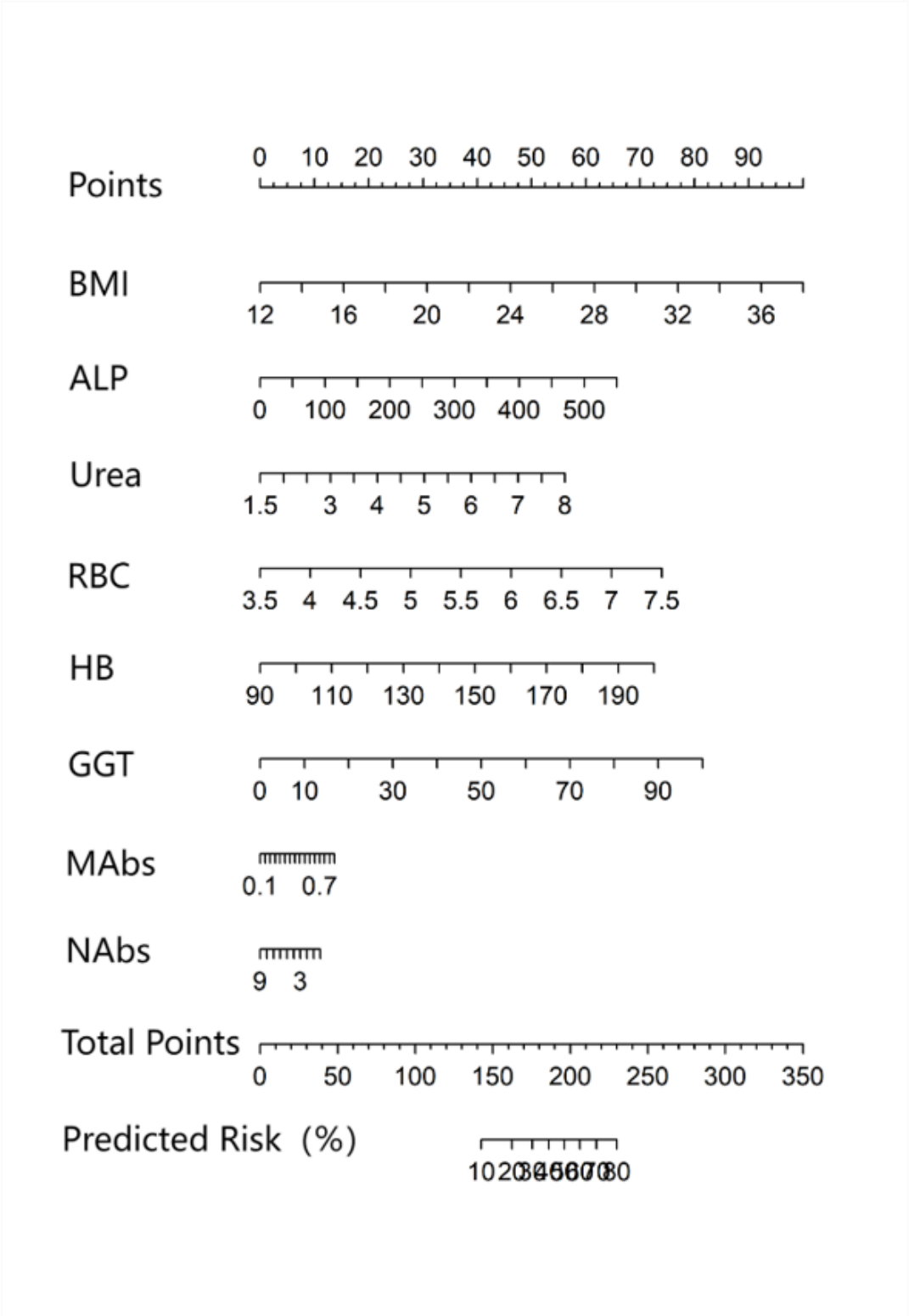


Figure 5

Static nomogram for predicting the risk of hyperuricemia in adolescents.
A static nomogram constructed from the multivariable logistic regression model incorporating body mass index (BMI), alkaline phosphatase (ALP), urea, red blood cell count (RBC), hemoglobin (HB), γ-glutamyl transferase (GGT), absolute neutrophil count (NAbs), and absolute monocyte count (MAbs). The total score corresponds to the estimated individual probability of hyperuricemia.

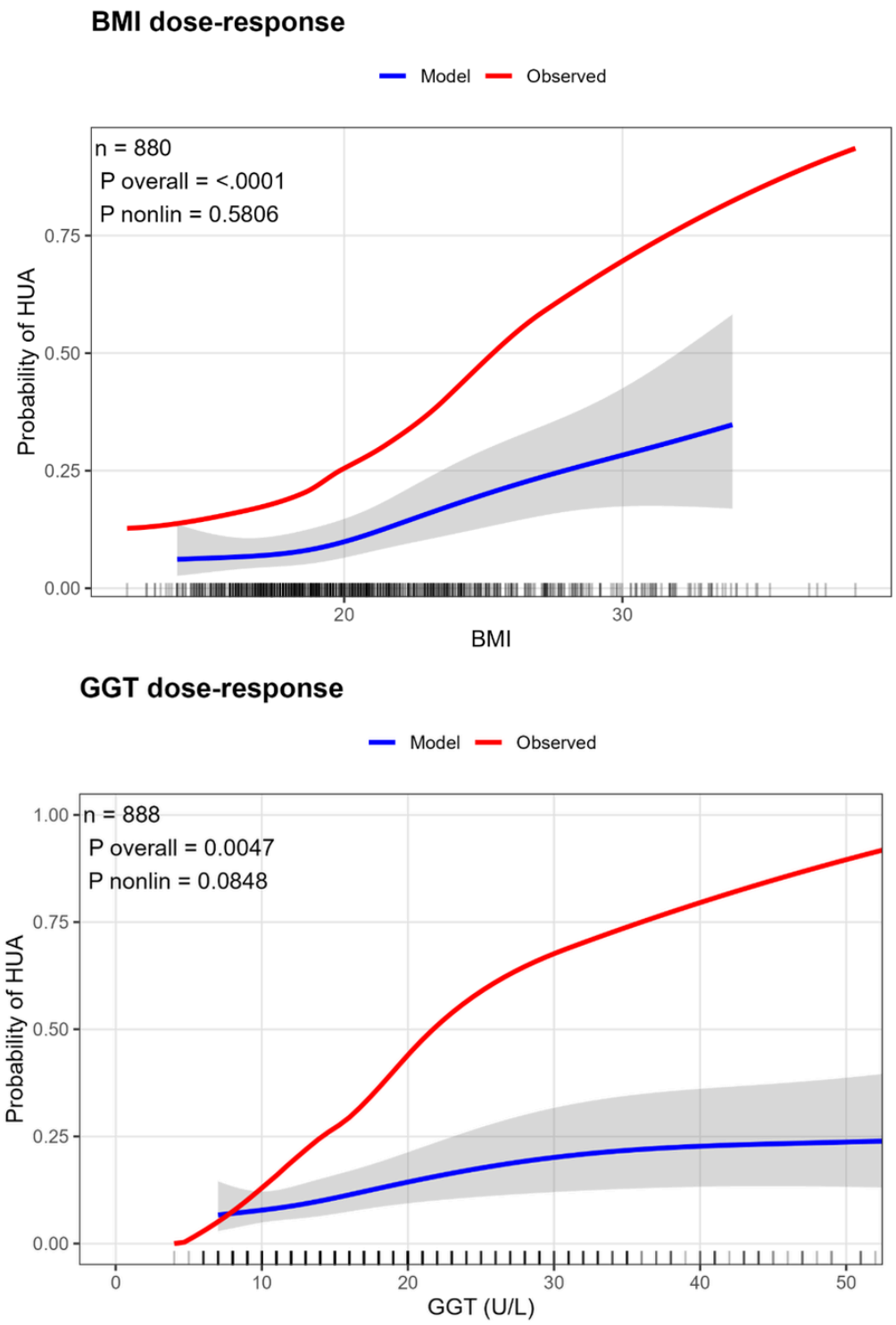


Figure 6

Restricted cubic spline analysis of BMI and GGT.

Restricted cubic spline curves showing the dose–response relationships between BMI, GGT, and the risk of hyperuricemia. BMI showed a significant positive linear association with hyperuricemia risk, whereas GGT was also positively associated with risk and showed a marginal nonlinear trend.

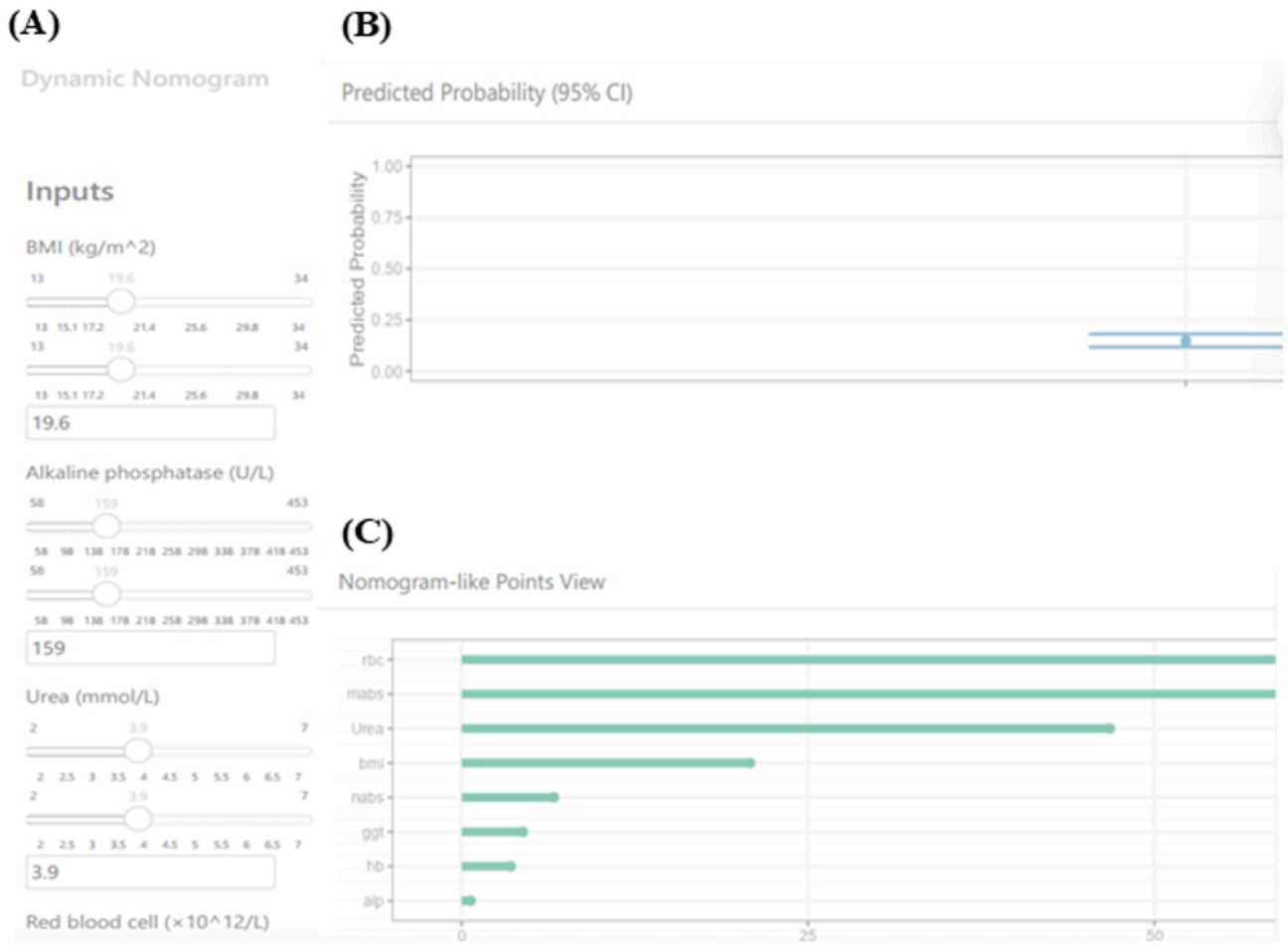


Figure 7

Web-based dynamic nomogram for individualized risk prediction.
(A) Overall interface of the dynamic nomogram allowing user-defined input of clinical variables.
(B) Visualization of the relative contribution of each predictor under the current input values.
(C) Output of individualized predicted risk with the corresponding 95% confidence interval.

Supplementary Files

This is a list of supplementary files associated with this preprint. Click to download.

- internalcalibration100.pdf
- externalcalibration100.pdf
- SupplementaryFigureS1.docx